I. Campos-Silva*, O. Franco-Raudales, J. A. Meda-Campaña, F. P. Espino-Cortés and J. C. Acosta-Pavón

Growth Kinetics of CoB–Co_2B Layers Using the Powder-Pack Boriding Process Assisted by a Direct Current Field

https://doi.org/10.1515/htmp-2018-0013
Received January 24, 2018; accepted May 22, 2018

Abstract: New results about the growth kinetics of CoB–Co_2B layers developed at the surface of CoCrMo alloy using the powder-pack boriding process assisted by a direct current field (PBDCF) were estimated in this work. The PBDCF was conducted at temperatures of 1048 – 1148 K with different exposure times for each temperature, whereas the growth kinetics of the cobalt boride layers was modelled using a system of two differential equations. In addition, indentation properties such as hardness, Young's modulus and residual stresses were estimated along the depth of the borided CoCrMo surface. The growth kinetics of the cobalt boride layers developed by PBDCF indicated that thicker boride layers were formed on the material's surface which was in contact to the current field at the anode, in contrast to the surface exposed at the cathode. The kinetics of cobalt boride layers were compared with those obtained by conventional powder-pack boriding process.

Keywords: powder-pack boriding, direct current field, cobalt boride layer, growth kinetics, depth-sensing indentation

PACS® (2010). 64.10.+h, 64.30.+t, 68.35.Fx, 72.15.Eb, 62.20.-x

***Corresponding author: I. Campos-Silva,** Grupo Ingeniería de Superficies, SEPI-ESIME, Instituto Politécnico Nacional, U.P. Adolfo López Mateos, Zacatenco, Ciudad de México, 07738, México, E-mail: icampos@ipn.mx
O. Franco-Raudales: E-mail: olivierfranco33@gmail.com, **J. A. Meda-Campaña:** E-mail: jmedac@ipn.mx, Grupo Ingeniería de Superficies, SEPI-ESIME, Instituto Politécnico Nacional, U.P. Adolfo López Mateos, Zacatenco, Ciudad de México, 07738, México
F. P. Espino-Cortés, Electrical Engineering Department, SEPI-ESIME, Instituto Politécnico Nacional, U.P. Adolfo López Mateos, Zacatenco, Ciudad de México, 07738, México, E-mail: fpespino@gmail.com
J. C. Acosta-Pavón, Grupo Ingeniería de Superficies, SEPI-ESIME, Instituto Politécnico Nacional, U.P. Adolfo López Mateos, Zacatenco, Ciudad de México, 07738, México,
E-mail: jc_acosta21@hotmail.com

Introduction

Boriding is a thermochemical treatment that increases the wear and corrosion resistance of ferrous and non-ferrous alloys by forming hard boride layers at the surface of the material [1]. In recent years, research on the boriding of cobalt alloys has advanced, specifically regarding the wear and oxidation properties of the cobalt boride layers [2–4]. In addition, the growth kinetics, some indentation properties, micro-abrasive wear resistance of CoB–Co_2B, and the practical adhesion resistance of the cobalt boride layers formed on the surface of the CoCrMo alloy by means of the conventional powder-pack boriding (CPBP) process have been estimated [5–7].

During the last ten years, the powder-pack boriding process assisted by a direct current field (PBDCF) has been studied in different grades of steels in order to produce boride layers on low temperatures (823 – 1023 K) with shorter exposure times (from 4 to 6 h) [8–11]. Traditionally, different setups have been proposed during the PBDCF, in which the steels have been positioned closely to the cathode and anode, or the materials were used as cathode and anode considering an applied current to the electrodes between 0.5 and 4 A. The steels were embedded in a closed-cylindrical container in contact with a powder mixture of B_4C, SiC and KBF_4. The results showed that the direct current field has different effects on the samples located at different positions in the closed-cylindrical container; in most of the cases, the growth of the boride layers on the material surface exposed to the current field at the anode was higher in comparison to the reversed surface.

In this study, the CoCrMo alloy was borided using the PBDCF process developed CoB–Co_2B layers at 1,098–1,148 K with different exposure times. The kinetics of the cobalt boride layers was estimated using a diffusion model proposed by Dybkov *et al.* [12], which considers a system of two differential equations to obtain the growth constants of both CoB and Co_2B. The results of the growth constants obtained by the diffusion model were expressed as Arrhenius relationships in the set of

experimental temperatures to verify the effect of the current field on the activation energies of boron in the CoB and Co_2B. Finally, the distribution of hardness, the Young's modulus, and the state of residual stresses along the cobalt boride layers obtained by the PBCDF process was estimated using the depth-sensing Vickers microindentation test.

Experimental procedure

The PBDCF process

Samples of CoCrMo alloy with 19 mm OD and 5-mm long were used in this study. The nominal chemical composition of the samples complying with the Micro-Melt BioDur Carpenter CCM Alloy standard is (mass %): C 0.14 max, Cr 26–30, Mo 5–7, Ni 1.0 max, Si 1.0 max, Mn 1.0 max, Fe 0.75 max, N 0.25 max and Co as balance. Before to the thermochemical treatment, the samples were ground sequentially using 100–2,000 grit SiC papers, polished and ultrasonically cleaned in an acetone solution for 15 min. The PBDCF process was accomplished by placing two electrodes (see Figure 1), with a separation of 10 mm, at the top of the lid of a steel container (AISI 304), that contains a powder mixture of 90 % B_4C as the donor, and 10 % KBF_4 as the activator. The CoCrMo samples were embedded in the powder mixture, and were positioned between the two electrodes, in which the anode electrode and the cathode electrode were respectively connected to the positive and negative output terminals of a regulated DC source. The container, with all the components, was heated in a conventional muffle, and the samples were placed under the influence of an electric field produced by a pair of electrodes inside the container.

The process was carried out at 1048, 1098 and 1148 K with exposure times of 0.5, 1, 1.5 and 2 h for each temperature. When the temperature is raised, a constant direct current field of 10 V and 4 A was applied between the two electrodes. After the treatment was complete, the container was slowly cooled at room temperature.

After the PBDCF process, the samples were subjected to metallographic characterization according to the method proposed by Bravo-Bárcenas *et al.* [7], in order to reveal the microstructure of the cobalt boride layer.

The thickness of cobalt boride layers was measured in clear field by optical microscopy with the aid of a GX51 Olympus instrument. Fifty measurements from a fixed reference (i. e., the borided surface) were made on four different sections of borided samples to determine the mean values of the boride layer thicknesses (CoB and Co_2B).

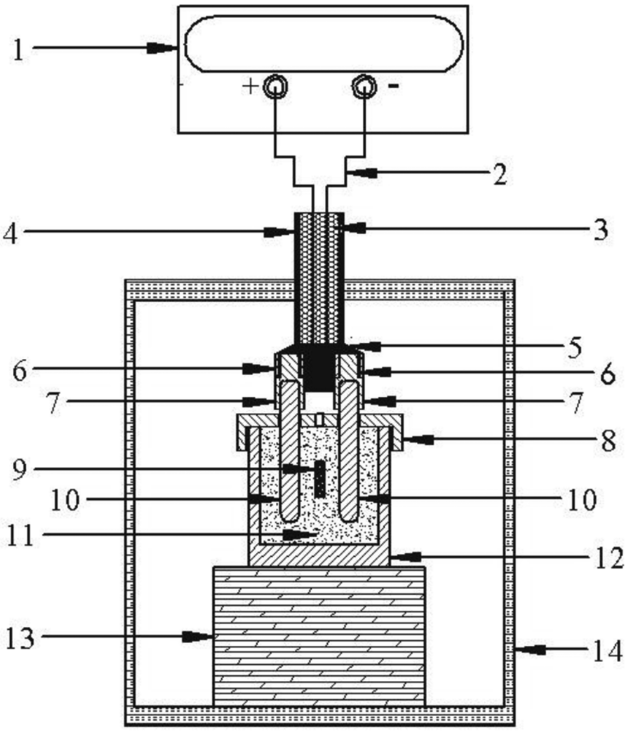

Figure 1: Schematic representation of the PBDCF system. 1: DC supplier, 2: Conducting wire, 3 and 4: Ceramic fiber insulation, 5: Refractory cement insulation, 6: Casing, 7: Connectors to electrodes, 8: Lid, 9: Sample, 10: Electrodes, 11: Boron powder mixture, 12: Container, 13: Partition refractory, 14: Muffle.

Finally, X-ray diffraction (XRD) was conducted on the surface of the borided sample exposed to the current field at the anode (1148 K with 2 h of exposure) to characterize the nature of compounds developed by the PBCDF method; a GBC Difftech XRD instrument (CuK_α radiation at $\lambda = 0.154$ nm) was employed. The collected data were analyzed and edited by the aid of the commercial Match 2.0 Crystal Impact Software. The software contains the JCPDS (Joint Committee of Powder Diffraction Standards) database to identify the compounds on the surface of borided cobalt alloy.

Depth-sensing microindentation tests

The borided CoCrMo alloy obtained at 1148 K with 1.5 h of exposure (anode and cathode) were tested on a commercial microindenter (UMT-2, Bruker Instruments) with a Vickers diamond indenter (Poisson's ratio = 0.07, Young's modulus $(E = 1141\,\text{GPa})$, in order to estimate the nature of residual stresses along the depth of CoB and

Co_2B. A constant indentation load of 200 mN (P_{max}) was used for this purpose, considering 7 microns approximately from the free surface and the same distance between indentations, enough to guarantee the correct results of depth-sensing microindentation. The indentation loads were performed in both surfaces exposed to the current field (anode and cathode), respectively. Likewise, Vickers indentations were performed in a direction perpendicular to the CoB–Co_2B-substrate interphase, which eliminated the potential for contributions from the substrate without restricting the maximum depth to 10 % of the total layer thickness.

For a particular distance from the surface of the borided CoCrMo alloy, three load–displacement curves were recorded automatically with the aid of the CETR software as shown in Figure 2. In first instance, the load–displacement curves were used to determine the hardness (H) and Young's modulus (E) of the cobalt boride layers.

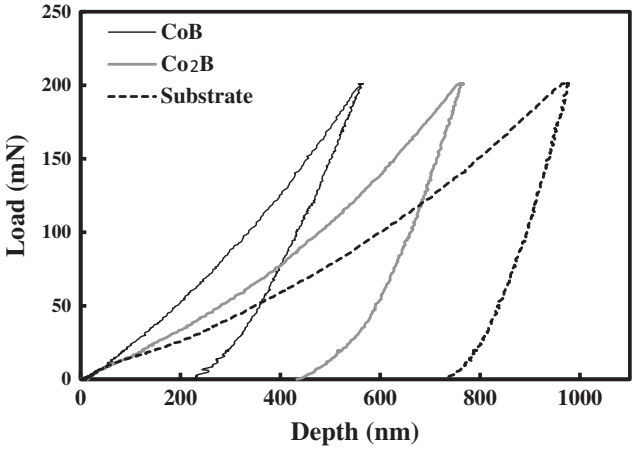

(a)

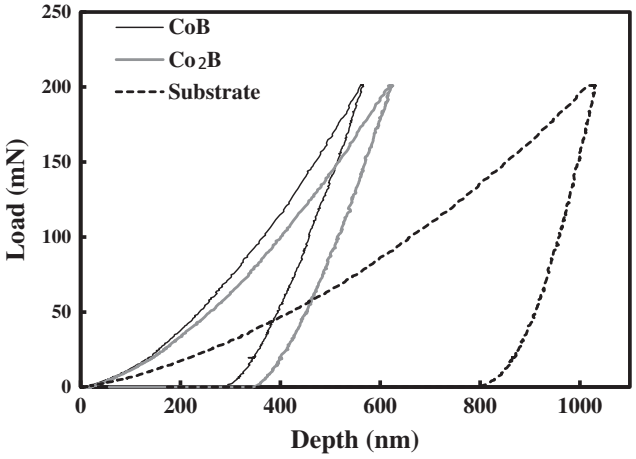

(b)

Figure 2: The depth-sensing Vickers microindentation: (a) load–displacement plots obtained on the cobalt boride layers developed at the surface exposed to the anode, and (b) load–displacement plots obtained on the cobalt boride layers developed at the surface exposed to the cathode. The CoB–Co_2B layers were developed at 1148 K with 2 h of exposure.

Results and discussion

Microstructure of the cobalt boride coating

Cross-sections of the CoCrMo alloy borided at 1048 and 1148 K with exposure times of 0.5 and 2 h for each temperature are presented in Figure 3. The surfaces of the CoCrMo exposed to the current field at the anode and cathode revealed the presence of flat CoB–Co_2B layers with a relative thin diffusion zone beneath the layers. The cobalt boride layers are developed by the following chemical reactions [8]:

$$KBF_4 = BF_3 + KF \quad (1)$$

$$2BF_3 + B_4C = 3BF_2 + 3[B] + C \quad (2)$$

On the material's surface, the gas BF_2 is ionized to B^{2+} and $[BF]^+$ by the direct current field, and the chemical reaction continues with diffusion of cobalt borides into the CoCrMo substrate, thus:

$$3BF_2 = [B] + 2BF_3 \quad (3)$$

$$[B] + 2Co = Co_2B \quad (4)$$

$$[B] + Co_2B = 2CoB \quad (5)$$

The electric field produces a current that flows between the two electrodes due to the electrical conductivity of the boriding agent (powder mixture) (see Figure 4). This current follows the direction of the field and passes through the sample. The field lines are perpendicular to the sample surface, with a direction into the surface at the side facing the anode and with a direction out of the surface at the side facing the cathode. Inside the sample, the electric field can be considered zero due to the high electrical conductivity of the material. The passage of electric current, which drives positive boron ions developed from the decomposition and chemical reaction of powder mixture, can either enhance or retard the growth of cobalt boride layers in the CoCrMo sample depending upon the flow

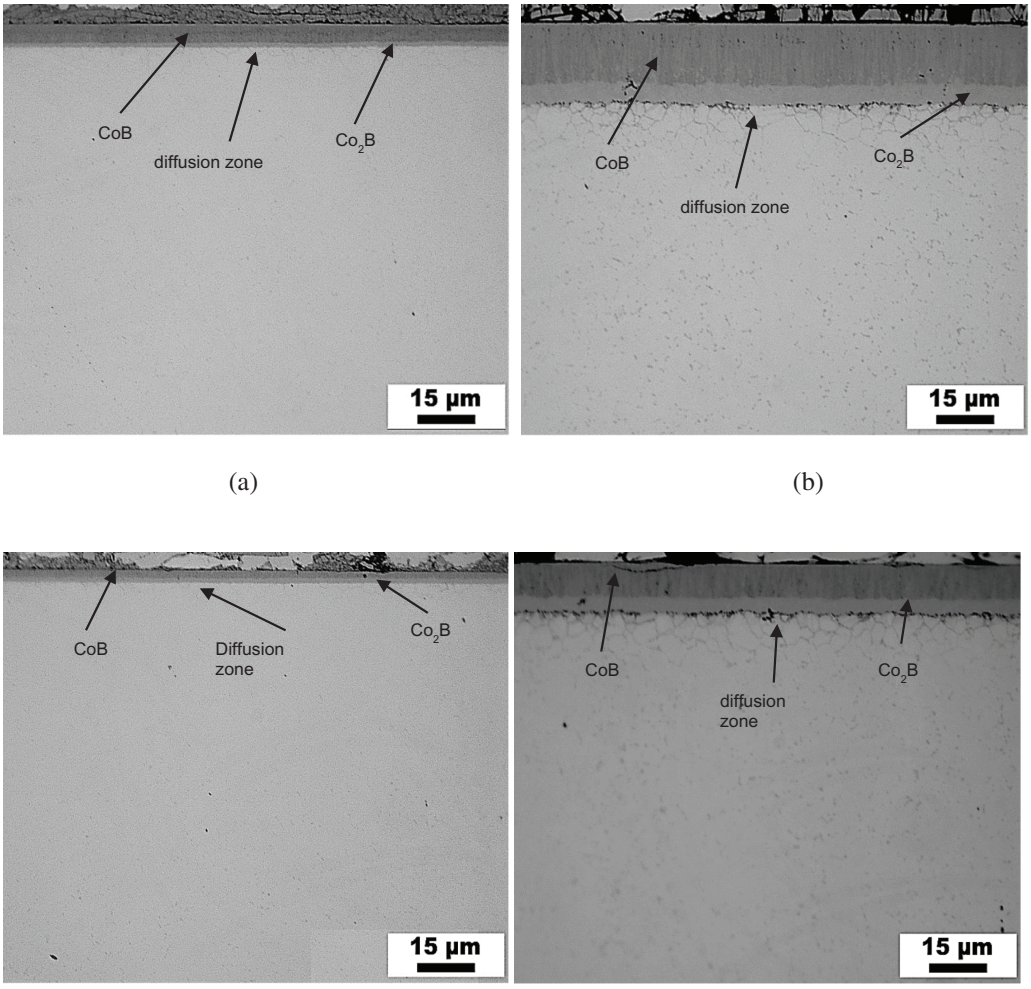

Figure 3: The CoB–Co_2B layers obtained on the side facing the anode with boriding conditions of: (a) 1048 K with 0.5 h of exposure, (b) 1148 K with 2 h of exposure. The microstructure of cobalt boride layers developed on the surface exposed to the cathode at: (c) 1048 K with 0.5 h of exposure, (d) 1148 K with 2 h of exposure.

directions of the electrons [8, 13]. At the anode, the mean values of the CoB layer thickness were ranged between 4 ± 0.3 μm for a PBDCF temperature of 1048 K with 0.5 h of exposure to 14 ± 0.3 μm for a temperature of 1148 K with 2 h of exposure; for the (CoB + Co_2B) layer thicknesses, the mean values were ranged between 5.5 ± 0.2 μm to 19 ± 0.5 μm, respectively. At the cathode, the cobalt boride layer thicknesses were decreased from 1.5 ± 0.3 μm to 9.1 ± 0.3 μm (CoB layer), and from 3 ± 0.3 μm to 12 ± 0.4 μm for the (CoB + Co_2B) layer, according to the extreme conditions of the PBDCF process.

According to the thickness of the boride layers resulting from the PBDCF process, the passage of electric currents in the CoCrMo sample enhanced the growth of CoB–Co_2B layer at the anode when the flow of electrons and the diffusional flow of boron are in the same direction; the passage of electric currents inhibited the growth of the cobalt boride layer at the cathode when the two directions are opposite.

It has been established that the direct current field supplies extra energy and improves the chemical reactions and decomposition of the powder mixture [14], that increases the boron potential (and the amount of active boron ions as well as atoms) surrounding the material's surface. This effect also causing the increase of mobility of point defects in the material, thus aiding mass transfer and enhancing layer growth in comparison with the CPBP process.

When a boron concentration is reached at certain points on the surface of the CoCrMo alloy, Co_2B crystals begin to nucleate, and a surface layer composed of Co_2B is

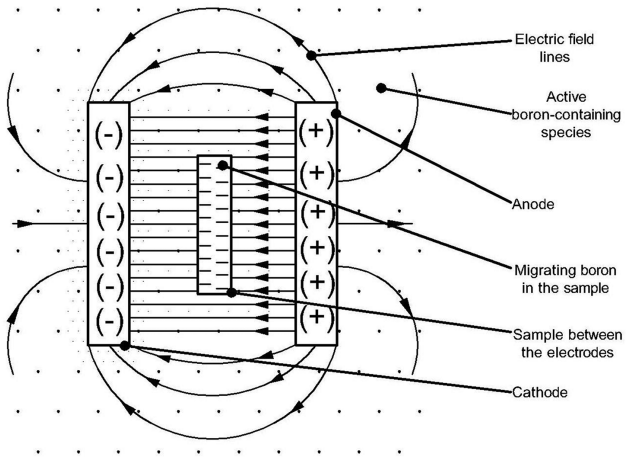

Figure 4: Schematic representation of boron mobility and electric field lines during the PBDCF (Modified from Xie *et al.* [8]).

formed. The flux of boron continues during the process but is restricted by the formation of a diffusion barrier composed by alloying elements of the substrate such as Ni, Cr, Mo, that rejected the boron to the surface, increasing the boron concentration and promoting the formation of the CoB layer on the outermost part of the sample. In both cases, the speed of boron diffusion in Co_2B and CoB layers is restricted by the presence of alloying elements of the substrate, which causes the reducing of the boride layer thicknesses.

Furthermore, the alloying elements such as Ni, Cr and Mo promote the formation of boron-rich reaction products (underneath the cobalt boride layer and positioned along the grain boundaries of the substrate) that compete with cobalt to enter the boride layer [5–7, 15, 16], thereby forming chromium and molybdenum compounds as shown in Figure 5.

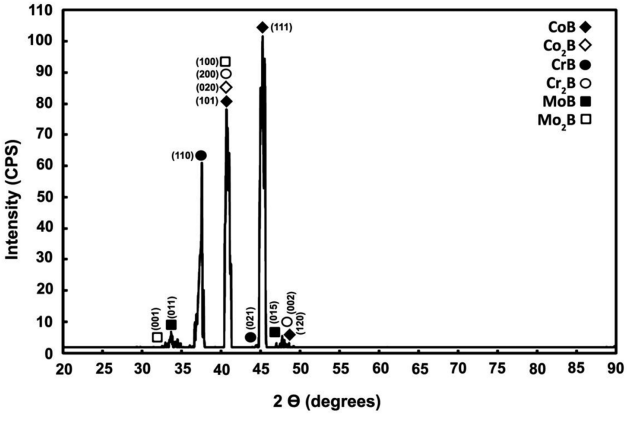

Figure 5: XRD pattern obtained on the borided CoCrMo alloy exposed to the anode. The PBDCF condition was 1148 K with 2 h of exposure.

Growth kinetics of CoB–Co_2B layers during the PBCDF process

Traditional diffusion models [17–19] suggest that the overall growth rate of boride layer obeys the parabolic law $X^2 = 2Kt$, where X is the mean thickness of the total boride layer, K is the growth rate constant, and t is the exposure time of the substrate to the boriding process. To estimate the boron activation energy in the boride layer (Q), the behavior of the growth rate constant as a function of the boriding temperature must be determined. Although the parabolic law is used to estimate the kinetics of boride layers, the results of Q are overestimated.

It has been established that the growth rate of both CoB and Co_2B interdepend [5, 20]. Thus, the estimation of the growth rate of CoB from kinetic parameters is possible only if the latter are known for both cobalt boride layers.

In this case, an alternative diffusion model for the estimation of the growth kinetics of boride layers proposed by Dybkov *et al.* [12] was adopted in this study. Basically, the model is related to the chemical reactions that occur at the growth interphase and the changes of thickness of the layers due to those reactions. In this case, the first phase that developed on the surface is Co_2B, which reacts with the boron and forming CoB. The CoB diffuses into the substrate and interacts with Co atoms, that diffuse from the substrate yielding the formation of Co_2B. Thus, the diffusion and interaction occur in two directions:

$$B + Co_2B \rightarrow 2CoB, \text{ and } CoB + Co \rightarrow Co_2B$$

The growth of boride layers at the diffusional stage of their formation can be described by a system of two nonlinear equations that account the evolution of the boride layers as a function of the exposure time. Hence:

$$\frac{dx}{dt} = \frac{k_{CoB}}{x} - \frac{rg}{p}\frac{k_{Co_2B}}{y} \tag{6}$$

$$\frac{dy}{dt} = \frac{k_{Co_2B}}{y} - \frac{q}{sg}\frac{k_{CoB}}{x} \tag{7}$$

where x and y are the boride layer thickness of the CoB and Co_2B, respectively, k_{CoB} is the growth rate constant of the CoB, k_{Co_2B} is the growth rate constant of the Co_2B, g is the ratio of the molar volumes of the CoB and Co_2B, $p = q = r = 1$, and $s = 2$ that are factors related to the chemical formulae of CoB and Co_2B [21]. Thus, eqs. (6) and (7) can be established as:

$$\frac{dx}{dt} = \frac{k_{CoB}}{x} - 0.5744\ \frac{k_{Co_2B}}{y} \tag{8}$$

$$\frac{dy}{dt} = \frac{k_{Co_2B}}{y} - 0.8658\ \frac{k_{CoB}}{x} \tag{9}$$

The model must be adjusted to the corresponding experimental parameters of the PBCDF process, considering the initial conditions: $x\ (0) = 1\times10^{-7}$m, $y\ (0) = 1\times10^{-7}$m.

In addition, the experimental measurement of the boride layers thicknesses (x and y) are used to obtain the respective growth velocities. This can be done by means of well-known expressions:

$$\frac{\Delta x}{\Delta t} = \frac{(\,(x(t) - x(t_p))}{(t - t_p)} \tag{10}$$

$$\frac{\Delta y}{\Delta t} = \frac{(\,(y(t) - y(t_p))}{(t - t_p)} \tag{11}$$

where $x\ (t)$ and $y\ (t)$ are the values of x and y at instant t, respectively, with t as the actual time and t_p as the previous time.

Once such velocities are computed ($\frac{\Delta_x}{\Delta_t}$, $\frac{\Delta_y}{\Delta_t}$) they are substituted in eqs. (8) and (9) transforming the dynamical model in a pair of simultaneous equations with two unknowns, namely, k_{CoB} and k_{Co_2B}. Thus, a solution for the mentioned simultaneous equations can be searched. Notice, that the discussed approach must be performed for every set of experimental data obtained in the different times of the PBDCF process. For that reason, it is necessary to compute the averages for k_{CoB} and k_{Co_2B}. Such averages are the growth constants needed by the model. At this point, the differential equations can be numerically solved by considering adequate initial conditions for the corresponding PBCDF process. In this work, the numerical solution of the mentioned model has been carried out in Matlab V. 9.1 through the toolbox SIMULINK 8.8.

Figure 6 shows the change of CoB and Co_2B layer thicknesses (simulated and experimental values) with respect of the PBCDF exposure time for the entire set of experimental conditions (anode and cathode). A reasonable agreement between the simulated data and the experimental data can be seen, in which the evolution of the cobalt boride layers formed on both sides of the CoCrMo sample exposed to the direct current field denoted a diffusion-controlled growth and indicating that the parabolic layer growth occurred. The values of k_{CoB} and k_{Co_2B} estimated from the boron diffusion in the

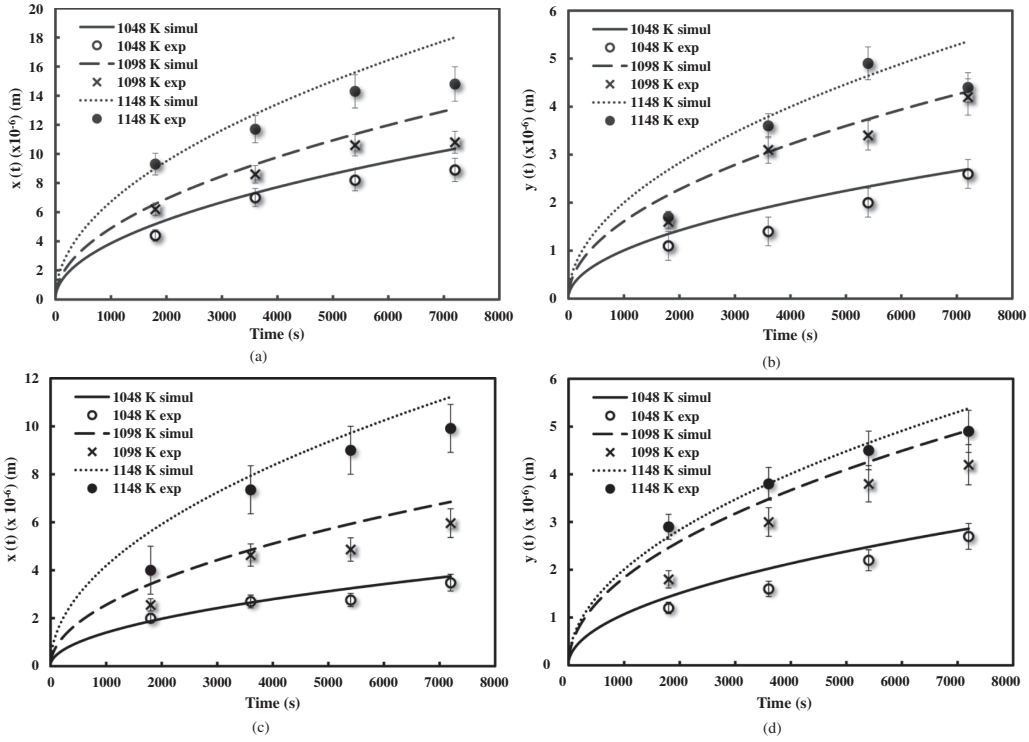

Figure 6: Evolution of CoB and Co_2B layers as a function of the exposure time during the PBDCF: (a) and (b) surface exposed at the anode, (c) and (d) surface exposed at the cathode.

Table 1: Estimated values of the growth constants obtained by the diffusion model.

Side facing direct current field	Temperature (K)	Exposure time ($\times 10^2$ s)	k_{CoB} ($\times 10^{-14}$ $\frac{m^2}{s}$)	k_{Co_2B} ($\times 10^{-14}$ $\frac{m^2}{s}$)
Anode	1048	18	3.10	2.68
		36	2.65	1.93
		54	1.66	1.37
		72	1.21	1.13
	1098	18	6.37	6.25
		36	3.50	3.54
		54	3.50	3.47
		72	1.22	1.86
	1148	18	13.6	10.8
		36	5.18	5.01
		54	6.06	5.54
		72	1.97	2.86
Cathode	1048	18	0.46	0.39
		36	0.43	0.38
		54	0.39	0.29
		72	0.16	0.10
	1098	18	1.02	0.80
		36	1.52	1.21
		54	0.35	0.42
		72	0.79	0.53
	1148	18	2.14	1.43
		36	3.72	2.13
		54	4.05	1.26
		72	2.20	0.92

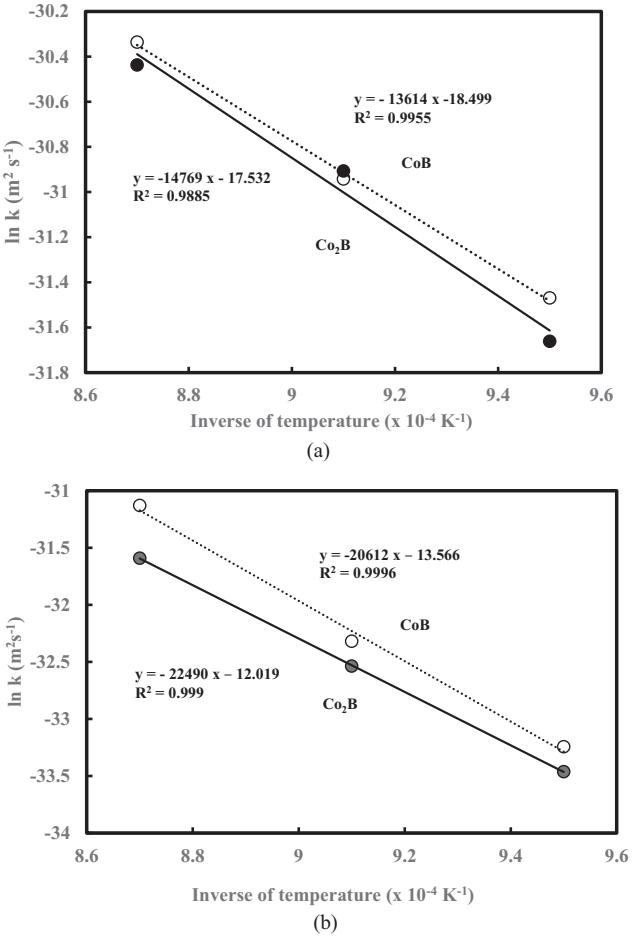

Figure 7: Temperature dependence of k_{CoB} and k_{Co_2B} according to the Arrhenius equation: (a) surface exposed at the anode, (b) surface exposed at the cathode.

CoB and Co_2B layers in both sides of the surface exposed to the direct current field are given in Table 1.

The average values of k_{CoB} and k_{Co_2B} estimated by the diffusion model were expressed as a function of the inverse of temperature according to the Arrhenius expression as shown in Figure 7. The boron activation energies in CoB and Co_2B estimated from the plots of Figure 7, for the overall PBDCF conditions, are summarized in Table 2. The results were compared with those obtained from the CPBP applied on the CoCrMo alloy [5].

It is evident that the influence of the current field enhances the mobility of boron in both CoB and Co_2B at the borided surface exposed at the anode in comparison with the surface at the side facing the cathode. In this case, at the anode, the flux of boron (perpendicular to the sample surface) and electrons are in the same direction [8] (see Figure 4). The activation energies of boron estimated at the cathode seem to be similar from those resulting from the CPBP in the range of temperatures of 1223 – 1273 K [5]. At the cathode, the migration of boron, resulted from the current field, is opposite to the normal diffusion boron direction increasing the activation energy of boron in CoB and Co_2B.

Table 2: Boron activation energies (Q) estimated in CoB and Co_2B layers.

Method	Layer	Q (kJ mol^{-1})	Pre-exponential factor (D_0) (m^2 s^{-1})	Range of boriding temperatures (K)	Reference
PBDCF (anode)	CoB	113 ± 10	9.2×10^{-9}	1048 ≤ T ≤ 1148	Present study
	Co_2B	123 ± 15	2.4×10^{-8}		
PBDCF (cathode)	CoB	171 ± 7	1.2×10^{-6}		
	Co_2B	187 ± 12	6.0×10^{-6}		
CPBP	CoB	189 ± 4	7×10^{-5}	1223 ≤ T ≤ 1273	[5]
	Co_2B	175 ± 5	3.3×10^{-6}		

Residual stresses in the CoB and Co_2B layers

According to the hardness results estimated along the depth of cobalt boride layers obtained at 1148 K with 2 h of exposure (Figure 8a), a maximum hardness (20 GPa) was obtained at 7 microns (CoB layer) from the free surface in both sides of the sample exposed to the direct current field; in the Co_2B layer a Vickers hardness value of 18 GPa was obtained, whereas on the substrate was of 5 GPa, approximately. Similarly, the distribution of the Young's modulus (E) in the CoB and Co_2B, at both sides of the surface exposed to the anode and the cathode, is

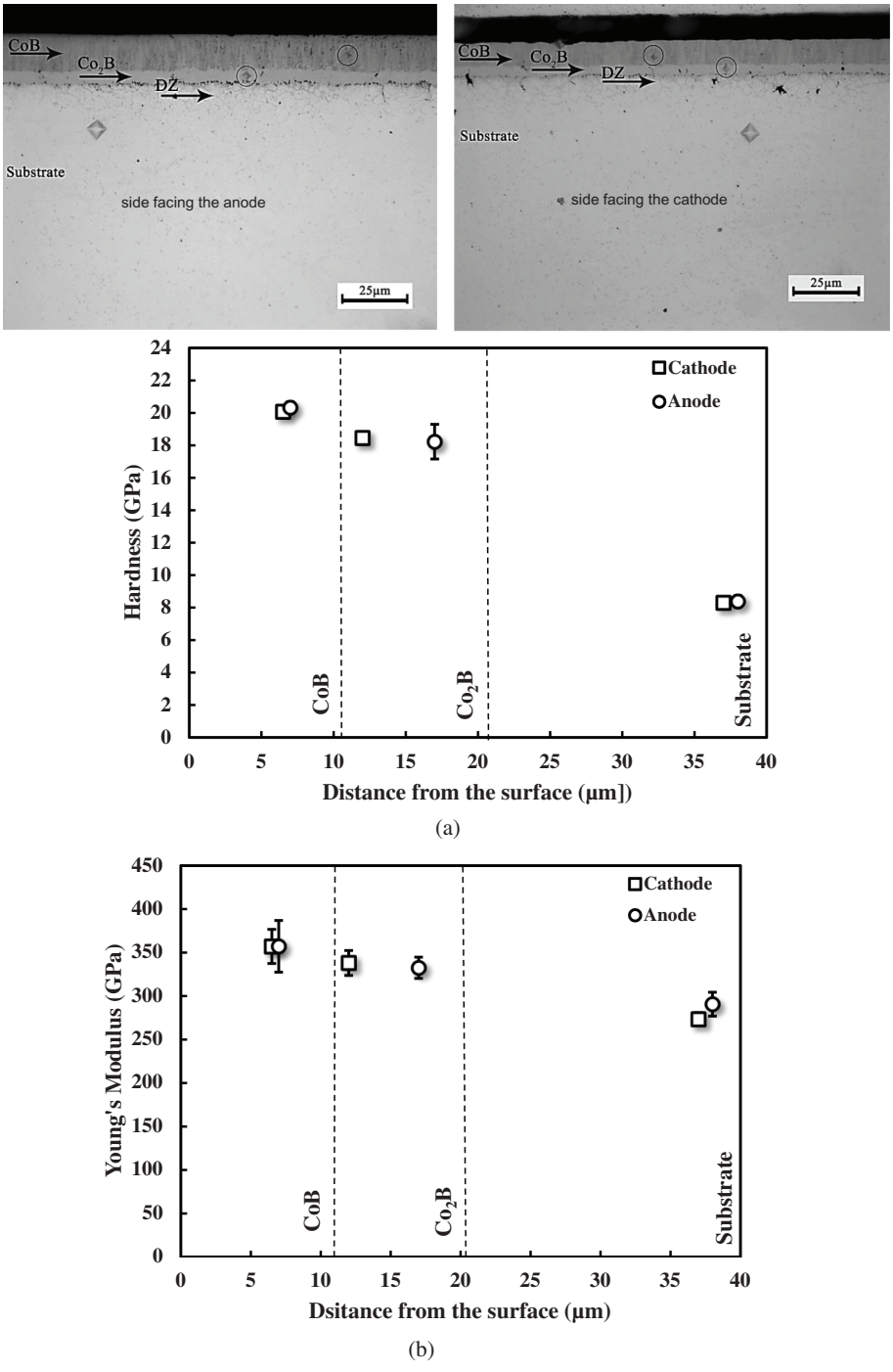

Figure 8: (a) Plots of the hardness-depth profiles across the cobalt boride layers developed at 1148 K with 2 h of exposure. (b) The Young's modulus (E) of the CoB and Co_2B against the distance from the borided surface. The PBDCF condition was 1148 K with 2 h of exposure.

shown in Figure 8b. A maximum E value of approximately 360 GPa near to the surface-region was estimated in the CoB (at the side facing the anode and cathode, respectively). In the Co_2B layer, the E values ranged between 332 GPa (anode) and 340 GPa (cathode), and gradually decreased, beneath the cobalt boride layer, to values between 273 to 290 GPa.

Moreover, given the values of Young's modulus obtained by depth-sensing Vickers microindentation, the residual stresses across the cobalt boride layers can be estimated from the expression proposed by Chen *et. al* [22].:

$$\frac{P}{E\,h^2} = 5.626\left(\frac{Y^*}{E}\right)^{0.5} \left\{1 - \left[3.51\left(\frac{Y^*}{E}\right)^{0.5} + 0.0032\left(\frac{Y^*}{E}\right)^{-0.5}\right]\left(\frac{\sigma_r}{Y^*}\right)\right\} \quad (12)$$

where $P = P_{max}$ is the maximum indentation load, h is the maximum indentation depth obtained from the load–displacement curve, Y^* is the yield stress of the cobalt boride layer Y = H/3 and σr is the residual stress. The mathematical expression (eq. (12)) was developed using dimensional analyses and finite element method for extracting materials properties from indentation measurements. When the residual stresses in surface layers is detected by indentation technique, the E/Y^* ratio should be smaller than 100 to ensure that the eq. (12) can be valid for materials.

Based on the results estimated from eq. (12) and presented in Figure 9, tensile residual stresses around 1.34 (at the anode) to 1 GPa (at the cathode) were estimated on the CoB layer, while compressive state between 1.16 and 1.38 GPa, (depending of the surface exposed to the direct current field) was dominant in the Co_2B layer. Furthermore, beneath the cobalt boride layer the stresses switched from compressive to tensile. Residual stresses are generated as a result of growth mechanisms, or in this case, specifically, by a mismatch in thermal expansion between the layers and CoCrMo substrate. The coefficient of thermal expansion of Co_2B ($\tilde{7}\times10^{-6}$ K^{-1}) is less than that of CoCrMo substrate ($\tilde{1}3.8\times10^{-6}$ K^{-1}) and hence, this phase remains in compression after cooling. The coefficient of thermal expansion of the CoB ($\tilde{2}0\times10^{-6}$ K^{-1}) is greater than the CoCrMo substrate or the Co_2B and therefore, remains in tension [23]. Also, the difference of Young´s modulus of the cobalt boride layers, the presence of cracks and porosity cause larger gradients along the depth of the CoB–Co_2B layer. The state of residual stresses estimated on the cobalt boride layers is comparable with those reported in the literature for the CoB and Co_2B layers obtained by the CPBP [7].

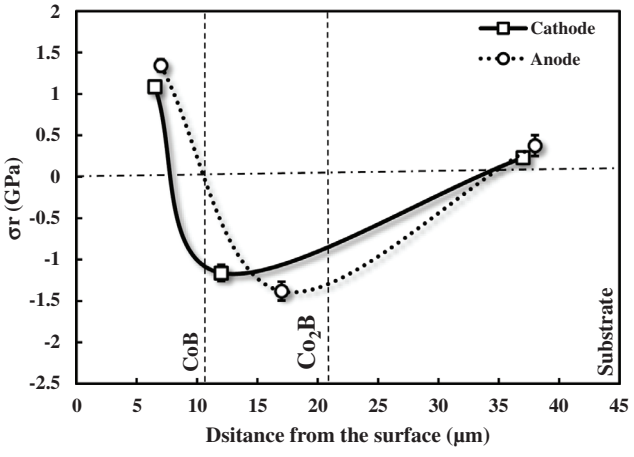

Figure 9: Distribution of the residual stresses along the depth of the cobalt boride layers. The PBDCF condition was 1148 K with 2 h of exposure.

Conclusions

New data about the growth kinetics of CoB–Co_2B layers subjected to the powder-pack boriding process assisted by a direct current field were estimated. were estimated. The growth constants for each cobalt layer were estimated by means of an alternative diffusion model that considers a system of non-linear differential equations. In this case, the evolution of the CoB–Co_2B layers as a function of exposure time, on the surface exposed at the anode and cathode, showed good agreement with the results display by the diffusion model. Moreover, for the entire set of PBDCF conditions, the results denoted that the CoB–Co_2B thicknesses were dissimilar on both sides of the surface exposed to the direct current field; the boron mobility at the surface exposed to the anode was increased and accelerated the formation of the CoB–Co_2B layers in comparison with the surface exposed at the cathode. Finally, according to the depth-sensing Vickers microindentation tests, the distribution of residual stresses in the CoB and Co_2B was verified; tensile residual stresses in the order of 1 GPa was estimated in the CoB whereas compressive stresses ranged between 1.1 and 1.3 GPa (independent of the surface exposed to the direct current field) were obtained in the Co_2B layer.

Acknowledgements: This work was supported by research grant 20180456 of the National Polytechnic Institute in Mexico.

References

[1] A.P. Krelling, J.C.G. Milan and C.E. da Costa, Surf. Eng., 31 (2015) 581–587.
[2] J.M. Johnston, M. Jubinsky and S.A. Catledge, Appl. Surf. Sci., 328 (2015) 133–139.
[3] D. Mu and S. Bao-Luo, Surf. Coat. Technol., 236 (2013) 102–106.
[4] G.A. Rodríguez-Castro, C.D. Reséndiz-Calderón, L.F. Jiménez-Tinoco, A. Meneses-Amador, E.A. Gallardo-Hernández and I.E. Campos-Silva, Surf. Coat. Technol., 284 (2015) 258–263.
[5] I. Campos-Silva, D. Bravo-Bárcenas, A. Meneses-Amador, M. Ortiz-Dominguez, H. Cimenoglu, U. Figueroa-López and J. Andraca-Adame, Surf. Coat. Technol., 237 (2013) 402–414.
[6] I. Campos-Silva, D. Bravo-Barcenas, H. Cimenoglu, U. Figuero-López, M. Flores-Jimenez and O. Meydanoglu, Surf. Coat. Technol., 260 (2014) 362–368.
[7] D. Bravo-Bárcenas, I. Campos-Silva, H. Cimenoglu, J. Martínez-Trinidad, M. Flores-Jiménez and H. Martínez-Gutierrez, Surf. Eng., 32 (2016) 570–577.
[8] F. Xie, L. Sun and J. Pan, Surf. Coat. Technol., 206 (2012) 2839–2844.
[9] F. Xie, Q. Zhu and J. Lu, Solid State Phenom., 118 (2006) 167–172.
[10] F. Xie and J.W. Pan, Int. Heat Treat. Surf. Eng., 6 (2012) 80–87.
[11] L. Angkurarach and P. Juijerm, Arch. Metall. Mater., 57 (2012) 799–804.
[12] V.I. Dybkov, L.V. Goncharuk, V.G. Khoruzha, A.V. Samelyuk and V.R. Sidorko, Mater. Sci. Technol., 127 (2011) 1502–1512.
[13] C.-M. Chen and S.-W. Chen, J. Electron. Mater., 28 (1999) 902–906.
[14] J. Garay, S.C. Glade, U. Anselmi-Tamburini, P. Asoka-Kumar and Z.A. Munir, Appl. Phys. Lett., 85 (2004) 573–575.
[15] I. Campos-Silva, D. Bravo-Bárcenas, M. Flores-Jiménez, I. Arzate-Vázquez, C. López-García and S. Bernabé-Molina, Metallogr. Microstruct. Anal., 4 (2015) 158–168.
[16] M.G. Krukovich, B.A. Prusakov and I.G. Sizov, Plasticity of Boronized Layers, Springer, Switzerland (2016).
[17] I. Gunes, M. Keddam, R. Chegroune and M. Ozcatal, Bull. Mater. Sci., 4 (2015) 1113–1118.
[18] Y. Kayali, I. Gunes and S. Ulu, Vacuum, 86 (2012) 1428–1434.
[19] I. Gunes and S. Kanat, Prot. Met. Phys. Chem. Surf., 51 (2015) 842–846.
[20] C.M. Brakman, A.W.J. Gommers and E.J. Mittemeijer, Mater. Res., 4 (1989) 1354–1370.
[21] V.I. Dybkov, Thermochemical Boriding of Iron-Chromium Alloys, IPMS Publications, Kyiv (2015).
[22] K.S. Chen, T.C. Chen and K.S. Ou, Thin Solid Films, 516 (2008) 1931–1940.
[23] P.A. Dearnley and T. Bell, Surf. Eng., 1 (1985) 203–217.